STEM CELLS AND DEVELOPMENT
Volume 24, Number 6, 2015

DOI: 10.1089/scd.2014.0255

Targeted Transplantation of Human Umbilical Cord Blood Endothelial Progenitor Cells with Immunomagnetic Nanoparticles to Repair Corneal Endothelium Defect

Chunyi Shao,* Junzhao Chen,* Ping Chen, Mengyu Zhu, Qinke Yao, Ping Gu, Yao Fu, and Xianqun Fan

Corneal endothelial dysfunction involves progressive corneal edema and loss of visual acuity, which result in the need for corneal transplantation. The global shortage of donor corneas limits the development of the surgery. Reconstruction of a bioengineered corneal endothelium might resolve this problem. Various scaffolds have been used, but poor biocompatibility and degradation limit their applications. In this study, a novel method of targeted cellular transplantation without permanent residence of cell carriers in the host was proposed. Human umbilical cord blood endothelial progenitor cells (UCB EPCs) were labeled with CD34 immunomagnetic nanoparticles. The efficiency of the magnet attraction was evaluated in vitro with a simple device simulating the anterior chamber. The UCB EPCs labeled with nanoparticles were transplanted into the anterior chamber of rabbits with magnet attraction. The results indicated that labeling the nanoparticles did not affect the proliferation of the UCB EPCs. The in vitro study indicated that the magnet could directionally attract UCB EPCs labeled with nanoparticles. The in vivo study indicated that the corneas in rabbits transplanted with UCB EPCs labeled with nanoparticles and magnet attraction became relatively transparent with little edema. These results showed that UCB EPCs labeled with CD34 immunomagnetic nanoparticles could be attracted directionally by a magnet and could repair corneal endothelial defects, providing a promising cell therapy for corneal endothelial dysfunction.

Introduction

It is estimated that there are 45 million individuals worldwide who are blind in both eyes. Corneal disease is a major cause of blindness in the world and remains second only to cataracts, with 1.5 to 2.0 million new cases of monocular blindness being reported every year [1]. Fuchs' dystrophy and bullous keratopathy are two common corneal endothelial diseases that involve progressive corneal edema and loss of vision, and these diseases require corneal transplantation, Descemet stripping automated endothelial keratoplasty, or Descemet membrane endothelial keratoplasty (DMEK). DMEK allows for the transplantation of an isolated endothelium–Descemet membrane layer (EDM) without adherent corneal stroma and provides faster and more complete visual rehabilitation [2]. However, the global shortage of donor corneas limits the transplantation. There is a great need to find new therapies to restore corneal clarity that is lost due to endothelial dysfunction. Reconstructing a bioengineered corneal endothelium might resolve this problem.

We previously proposed the performance of the transplantation of bone marrow endothelial progenitor cell (EPC)-derived corneal endothelial-like cells using porcine corneal acellular matrix to repair corneal endothelium defects, and we showed the effectiveness of this technique [3]. However, the porcine corneal acellular matrix did not degrade during the follow-up period. The residual presence of this material was responsible for the failure to obtain complete transparency of the cornea.

In the current study, we propose a novel method of target cellular transplantation without permanent residence of cell carriers in the host. Human umbilical cord blood endothelial progenitor cells (UCB EPCs) bound with immunomagnetic nanoparticles were transplanted into the rabbit chambers combined with magnetic attraction. The feasibility of this method was investigated.

Materials and Methods

UCB samples

The human UCB was obtained from the Tissue Bank Gynecology & Obstetric Hospital, Fudan University. The cord blood was collected from normal deliveries of full-term infants. Written informed consent was obtained from all the

Department of Ophthalmology, Ninth People's Hospital, Shanghai Jiao Tong University School of Medicine, Shanghai, China.
*These two authors contributed equally to this work.

mothers before delivery. The harvested volume was an average of 50 mL from a single placenta. The protocols for sampling human UCB were approved by the ethics committee of Shanghai Ninth People's Hospital, Shanghai Jiao Tong University School of Medicine. The study adhered to the tenets of the Declaration of Helsinki involving human subjects.

Culture of UCB EPCs

Mononuclear cells (MNCs) were isolated from fresh human UCB diluted with phosphate buffered saline (PBS; Gibco, Grand Island, NY) as 1:1, by Ficoll density-gradient centrifugation (1.077 g/mL; StemCell Technologies, Meylan, France) and washed twice with PBS containing 2% fetal bovine serum (FBS; Gibco). The MNCs were suspended in EGM-2 culture medium (Clonetics, Lonza, Walkersville, MD) [4] enriched with 10% FBS (HyClone, Logan, UT), hydrocortisone, hFGF-B, VEGF, R3-IGF-1, ascorbic acid, hEGF, and GA-1000 on collagen type I coated six-well plates [5] (Millipore, Billerica, MA) at 37°C in a 5% CO_2 humidified atmosphere. After incubation for 4 days, the nonadherent cells and debris were aspirated, and the adherent cells were cultured with EGM-2. The medium was changed every 2 days. The colonies were treated with 0.25% trypsin-EDTA (Gibco) at 9–11 days and plated in another six-well plate with EGM-2 medium containing 5% FBS for further passage.

Characteristics of human UCB EPCs

The identification of the ex vivo expanded UCB EPCS was performed as previously described. Briefly, adherent cells were incubated with 10 μg/mL 1,1′-dioctadecyl-3,3,3-tetramethylindocarbocyanine-labeled acetylated low-density lipoprotein (DiI-Ac-LDL; Invitrogen, Carlsbad, CA) at 37°C for 4 h and then counterstained with 10 μg/mL fluorescein isothiocyanate-conjugated lectin Ulex europeaus agglutinin-1 (UEA-1; Sigma-Aldrich, St. Louis, MO) at 37°C for 2 h. The results were evaluated using fluorescence microscopy (Olympus BX51, Tokyo, Japan) by two independent investigators [3].

Further characterization was performed using mouse monoclonal anti-CD133 (MAB4399; Millipore), rabbit polyclonal CD34 (sc-9095; Santa Cruz, Santa Cruz, CA) and rabbit polyclonal von Willebrand factor (vWF) (Abcam, Cambridge, MA) immunofluorescence staining. Briefly, UCB EPCS were cultured on glass coverslips (VWR, West Chester, PA) coated with fibronectin (Millipore) for 1 day and fixed in 4% (w/v) paraformaldehyde (Sigma-Aldrich) for 15 min at room temperature. The cells were washed with PBS and blocked for 1 h in a blocking solution [PBS containing 10% (v/v) normal goat serum (Invitrogen), 0.3% Triton X-100 (Sigma-Aldrich), and 0.1% NaN_3 (Sigma-Aldrich)]. The samples were incubated in the primary antibodies at 4°C overnight. After washing with PBS, fluorescent-labeled secondary antibodies (Alexa $Fluor^{546/488}$ goat anti-mouse/rabbit; BD Biosciences, San Jose, CA) were diluted 1:800 in PBS and applied for 1 h at room temperature. After washing, the cell nuclei were counterstained with Hoechst 33342 (Invitrogen). The negative control samples were processed in parallel without the primary antibody. Immunoreactive cells were visualized and the images were recorded using a fluorescent microscope (Olympus BX51). The quantification of the cells was based on counting the number of Hoechst-stained nuclei and immunoreactive cells in at least five independent fields, for a total of at least 500–1,000 cells [6,7]. The data was collected by Image-Pro Plus 6.0 (Media Cybernetics, Bethesda, MD), which is an automated software for counting.

Human UCB EPCs labeled with CD34 immunomagnetic nanoparticles

The UCB EPCs were magnetically labeled using the EasySep Human Cord Blood CD34 Positive Selection Kit according to the manufacturer's protocols (StemCell Technologies) [8]. Briefly, the second passage of UCB EPCs was suspended in 5 mL tube (BD Biosciences) with 100 μL of the recommended medium (2×10^8 cells/mL, PBS containing 2% FBS and 1 mM EDTA, free of Ca^{++} and Mg^{++}), and the EasySep Positive Selection Cocktail [contains a combination of monoclonal antibodies, which are bound in bispecific tetrameric antibody complexes (TAC), directed against CD34 and dextran] was added at 100 μL/mL. The solution was mixed well and incubated at room temperature for 15 min. The EasySep Magnetic Nanoparticles (a suspension of magnetic dextran iron particles in water) were added at 50 μL/mL cells, and the solution was mixed well and incubated at room temperature for 10 min. The cell suspension was brought to a total volume of 2.5 mL by adding the recommended medium. The cells were mixed by gently pipetting up and down two to three times. The tube was placed into the EasySep magnet and set aside for 5 min. The magnet was picked up, and the magnet and tube were inverted in one continuous motion, pouring off the supernatant fraction. The magnetically labeled cells remained inside the tube. The tube was removed from the magnet, and 2.5 mL of the recommended medium was added. The cells were mixed, and the tube was placed back into the magnet and set aside for 5 min. The supernatant fraction was poured off and the magnetically labeled cells remained inside the tube ready for use.

In vitro evaluation of cell proliferation after labeling with CD34 immunomagnetic nanoparticles

After labeling, CD34 was further tested by flow cytometry. The following monoclonal antibodies were used: anti-human CD34 and FITC-conjugated mouse IgG1 isotype control (eBioscience, San Diego, CA). The labeled cells were incubated with antibodies for 30 min at 4°C in the dark. The samples were then washed twice with buffer (PBS with 4% FBS) and resuspended with 200 μL buffer, which was ready for analyzing by a flow cytometer (Epics Altra; Beckman Coulter, Fullerton, CA).

The cell counting kit-8 (CCK-8) (Dojindo, Kumamoto, Japan) assay was used to test the cytotoxicity of the magnetic nanoparticles and cell proliferation [9]. Briefly, UCB EPCs P_2 with and without nanoparticle labeling were suspended at a final concentration of 5×10^3 cells per well and were cultured in two separate 96-well plates. At days 0, 1, 2, 3, 4, and 5 of the culture period, the CCK-8 solution was added to the corresponding well. After the cells were incubated for another 3 h at 37°C according to the reagent

instructions, the absorbance at 450 nm was measured using an ELISA microplate reader (ELX800; BioTeK, Winooski, VT). The cell viability is directly proportional to the absorbance at 450 nm, and the viability was expressed as the A450 value [6].

A cell proliferation marker, Ki-67 (mouse anti-human Ki-67; BD Biosciences), was examined in the UCB EPCs with or without CD34 immunomagnetic nanoparticles. The immunofluorescence protocol to detect Ki-67 is as described above [6].

Magnetic design

The magnet was a compound structure (Shanghai Te-Bearing Electronic Devices & Meter Parts Co. Ltd., Shanghai, China). The inner portion was made up of a Neodymium magnet, 3,500 gauss, with a diameter of 15 mm. The outer part was made of copper with an outer diameter of 20 mm. The magnet height was 8 mm.

In vitro attraction of UCB EPCs labeled with CD34 immunomagnetic nanoparticles with a magnet

The efficiency of the magnet attraction was tested in vitro with a simple device simulating the anterior chamber (Fig. 1). A 35-mm culture dish was used containing 6 mL of EGM-2 medium (5% FBS). The CD34 immunomagnetic nanoparticle-labeled UCB EPCs with a total number of 2×10^6 suspended in 2 mL EGM-2 were added in the culture dish and mixed well. An additional 1 mL EGM-2 was added to fill the culture dish. The culture dish was carefully covered, avoiding overflow of the medium. The culture dish was moved from the super clean bench evenly, and was quickly turned over with the thumb and forefinger holding the dish tightly. The dish was placed in a 10-cm culture dish for convenient shifting and to avoid contamination. The sterilized magnet was placed on the 35-mm culture dish. The cells were cultured in this device at 37°C in a 5% CO_2 humidified atmosphere. Different time periods of magnetic attraction were examined. In Group 1, after 2 h of culture, the magnet was removed, the medium with the nonadherent cells was discarded, and the adherent cells continued to be cultured with fresh EGM-2 in an inverted position. The observation time points were 2, 24, and 48 h. In Group 2, after 24 h of culture, the magnet was removed, the medium with the nonadherent cells was discarded, and the adherent cells continued to be cultured with fresh EGM-2 in an inverted position. The observation time points were 24 and 48 h.

Targeted transplantation of UCB EPCs with immunomagnetic nanoparticles in vivo

The New Zealand white rabbits were obtained from the Shanghai Animal Experimental Center, and all procedures were approved by the Animal Research Committee of Ninth People's Hospital, Shanghai Jiao Tong University School of Medicine.

The surgical procedure followed DMEK. New Zealand white rabbits weighing 2.0–2.5 kg were anesthetized with ketamine hydrochloride (10 mg/kg) and xylazine hydrochloride (6 mg/kg). After applying topical hydrochloric oxybuprocaine eye drops (Santen, Osaka, Japan), the central cornea was gently marked using a 9 mm trephine. A 2.5 mm puncture incision was made at the limbus at the 9 o'clock position with a 2.5 mm diamond knife. Surgery was performed on the right eye only, under an ophthalmic microscope (Leica M620 F18). Medical hyaluronan gel (Bausch Lomb, Rochester, NY) was injected to maintain the volume of the anterior chamber. The EDM was removed using an inverted hook inside the 9-mm marking [2]. The anterior chamber was washed with sodium lactate ringer's injection (Baxter, Irvine, CA) to remove the viscoelastic solution. The incision was sutured by 10-0 monofilament thread (Ethicon,

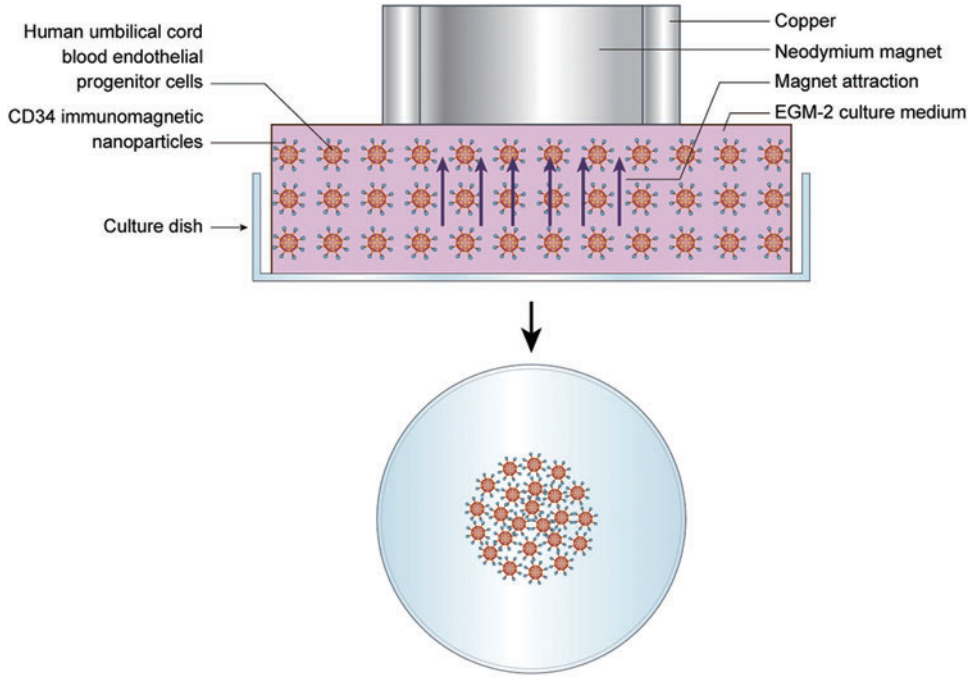

FIG. 1. Diagram of in vitro attraction of umbilical cord blood endothelial progenitor cells (UCB EPCs) labeled with CD34 immunomagnetic nanoparticles with a magnet and a simple device simulating the anterior chamber. Color images available online at www.liebertpub.com/scd

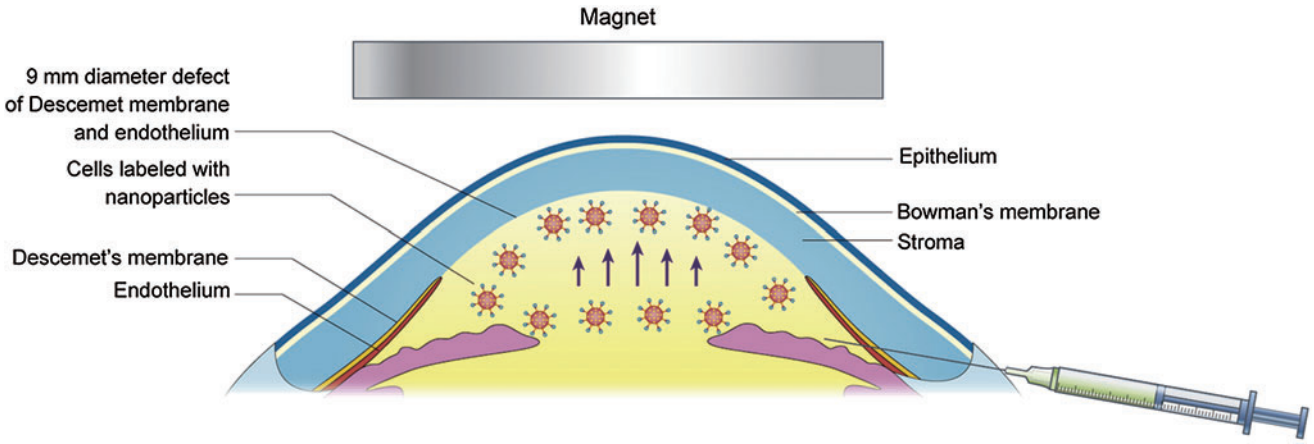

FIG. 2. Diagram of in vivo targeted transplantation of UCB EPCs labeled with CD34 immunomagnetic nanoparticles with magnet attraction. With the magnet attraction, the cells could migrate directionally (*blue arrows*). Color images available online at www.liebertpub.com/scd

Johnson & Johnson, Somerville, NJ). The UCB EPCs with CD34 immunomagnetic nanoparticles (4×10^5 cells in 100 μL EGM-2) tracked with CM-Dil (C700; Invitrogen) were injected into the anterior chamber with a 25-gauge needle at the 8 o'clock position (Fig. 2). The magnet was fixed on the eyelid with a bandage for 12 h to attract the UCB EPCS to the host corneal stroma.

Four groups of rabbits with four rabbits in each group were studied, including rabbits with CD34 immunomagnetic nanoparticle-labeled UCB EPCS and a magnet (nano group), CD34 immunomagnetic nanoparticle-labeled UCB EPCS without a magnet (control group), EDM stripping but no injection of cells (model group), and normal group.

Observations of transplanted corneas

The surgically treated eyes were examined weekly after surgery. The data were recorded at 2 weeks and 2 and 4 months by external examination with a slit lamp biomicroscope followed by photography. The corneal edema was classified as described by Mimura: 0, completely transparent cornea; 1, minimal corneal opacity, but iris vessels easily visible; 2, moderate corneal opacity, iris vessels still visible; 3, moderate corneal opacity, only pupil margin visible; 4, complete corneal opacity, pupil not visible [10]. The central corneal thickness (CCT) and anterior chamber angle were measured using the Zeiss Cirrus HD-OCT (Carl Zeiss Meditec, Inc., Dublin, CA). The intraocular pressure was measured by a rebound tonometer (SUOER SW-500, Shanghai, China). The endothelial density was measured by Topcon sp3000p noncontact specular microscopy (Topcon, Tokyo, Japan).

Histological examination of UCB EPCs

Four months after transplantation, the rabbits were anesthetized and killed by air injections into the ear vein. The corneas were excised and fixed in 4% paraformaldehyde for 18 h. The corneal paraffin sections were used for Hematoxylin and Eosin (HE) staining, mouse anti-human nuclei monoclonal antibody (MAB1281; Millipore) immunohistochemistry (IHC) staining (only for human cell nuclei staining, not reacting with nuclei from rabbit or mouse) [11] performed automatically by Leica BOND-MAX™ (IHC staining system), and Berlin blue staining (iron stain). The corneal cryosections were used for CM-Dil tracking and Aquaporin 1 (rabbit polyclonal AQP1, sc-20810; Santa Cruz) immunofluorescence staining, using the method described above.

Statistical analysis

All the data presented in this study are shown as the mean ± standard deviation. The *t*-test was used to compare CCK-8, Ki-67, and endothelial density. The general linear model was used to compare the corneal edema grading, corneal thickness, and intraocular pressure in different groups. *P*-values <0.05 were considered statistically significant.

Results

Characterization of UCB EPCs

Colonies of the UCB EPCs appeared between 4 and 6 days of culture, and the number and size increased quickly at 8 days of culture. The colony number per 10 mL of UCB on the fifth day was 20 ± 2 and increased to 64 ± 5 on the eighth day. The colony diameter on the fifth day was 0.90 ± 0.74 mm and increased to 1.56 ± 1.47 mm on the eighth day, and some colonies came to fusion. The morphology of the colonies was identified as well-circumscribed monolayers of cobblestone-appearing cells. After the UCB EPC passage, monolayers of short spindle cells formed (Fig. 3). The UCB EPCs could uptake Dil-Ac-LDL and bind endothelial specific lectin UEA-1. Additional staining revealed that the cells were positive for CD133, CD34, and vWF (Fig. 4).

Cell viability and proliferation after being labeled with CD34 nanoparticles

91.4% ± 4.0% of the isolated UCB EPCs expressed CD34 after labeling. To investigate the effect of the CD34 nanoparticles on UCB EPCs proliferation, the proliferation was evaluated by CCK-8 analysis. There were no significant differences in the proliferation of the UCB EPCs with

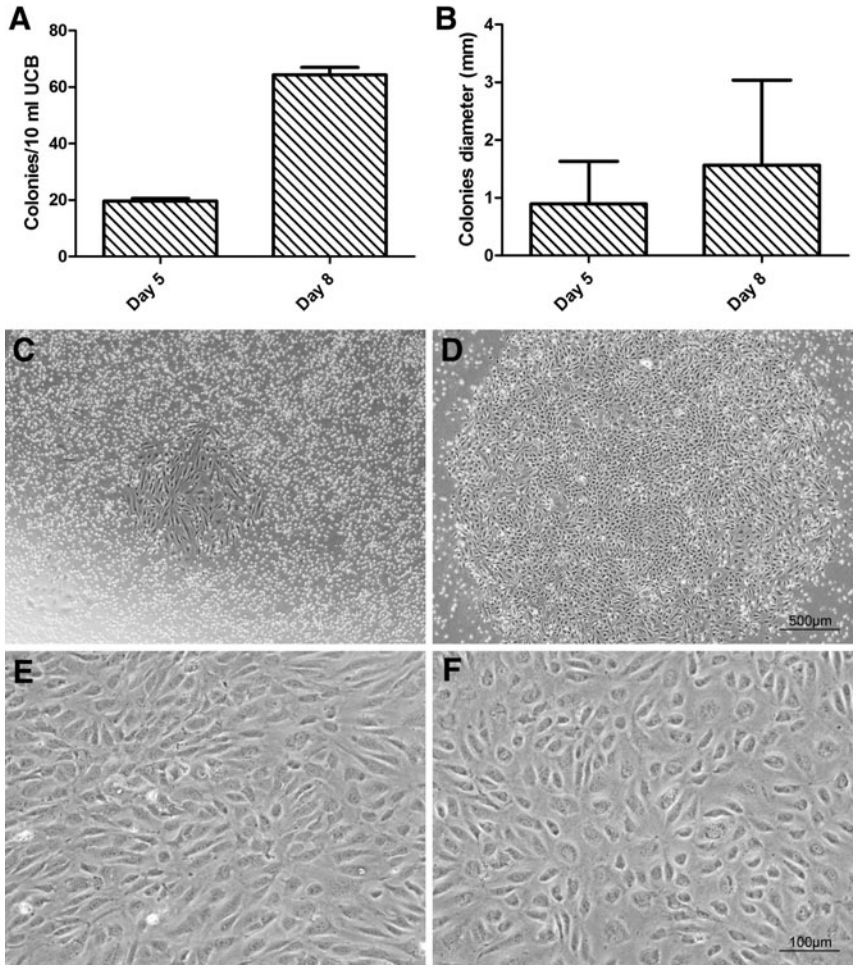

FIG. 3. The colonies and morphology of human UCB EPCs. **(A)** Colony numbers. The colony number per 10 mL human UCB on the fifth day was 20 ± 2 and increased to 64 ± 5 on eighth day. **(B)** Colony size. The colony diameter on the fifth day was 0.90 ± 0.74 mm and increased to 1.56 ± 1.47 mm on the eighth day. **(C)** Colony of 5 days of culture with small diameter. **(D)** The same colony after 8 days of culture (scale bar = 500 μm). **(E)** First passage of the UCB EPCs showed short spindle shape. **(F)** Second passage of the UCB EPCs (scale bar = 100 μm).

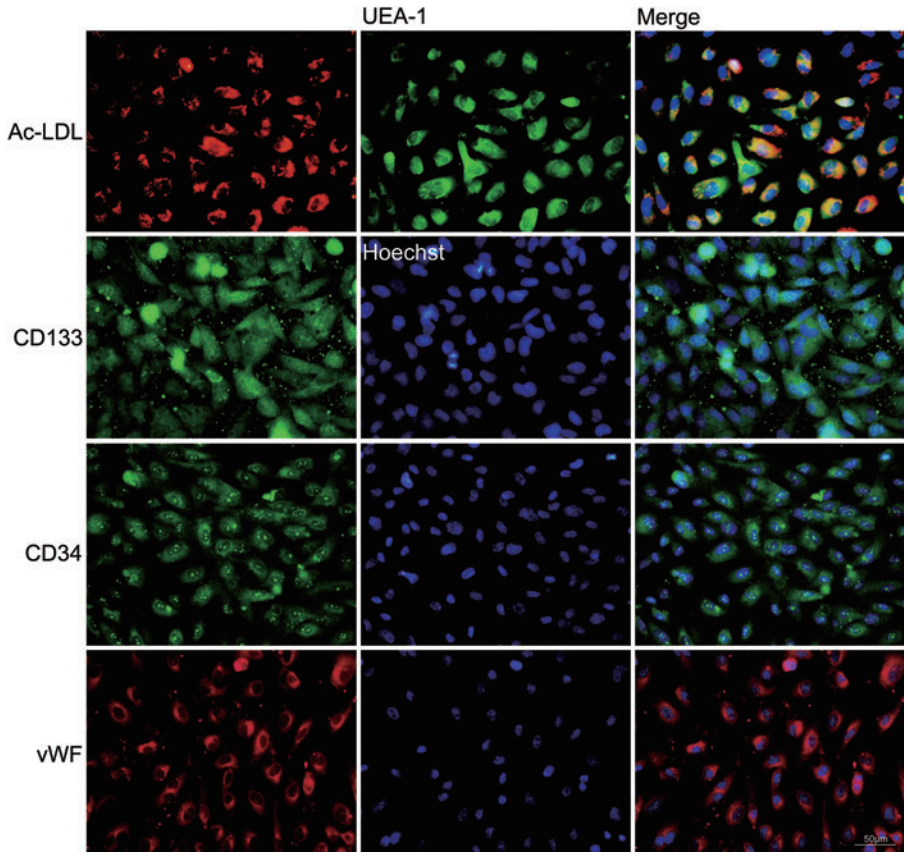

FIG. 4. Characterization of human UCB EPCs. The fluorescent micrograph showed that the UCB EPCs could take up Dil-Ac-LDL, (*red*), bind UEA-1 (*green*), and express CD133, (*green*), CD34, (*green*), and vWF (*red*). Nuclei were stained with Hoechst (*blue*) (scale bar = 50 μm). Color images available online at www.liebertpub.com/scd

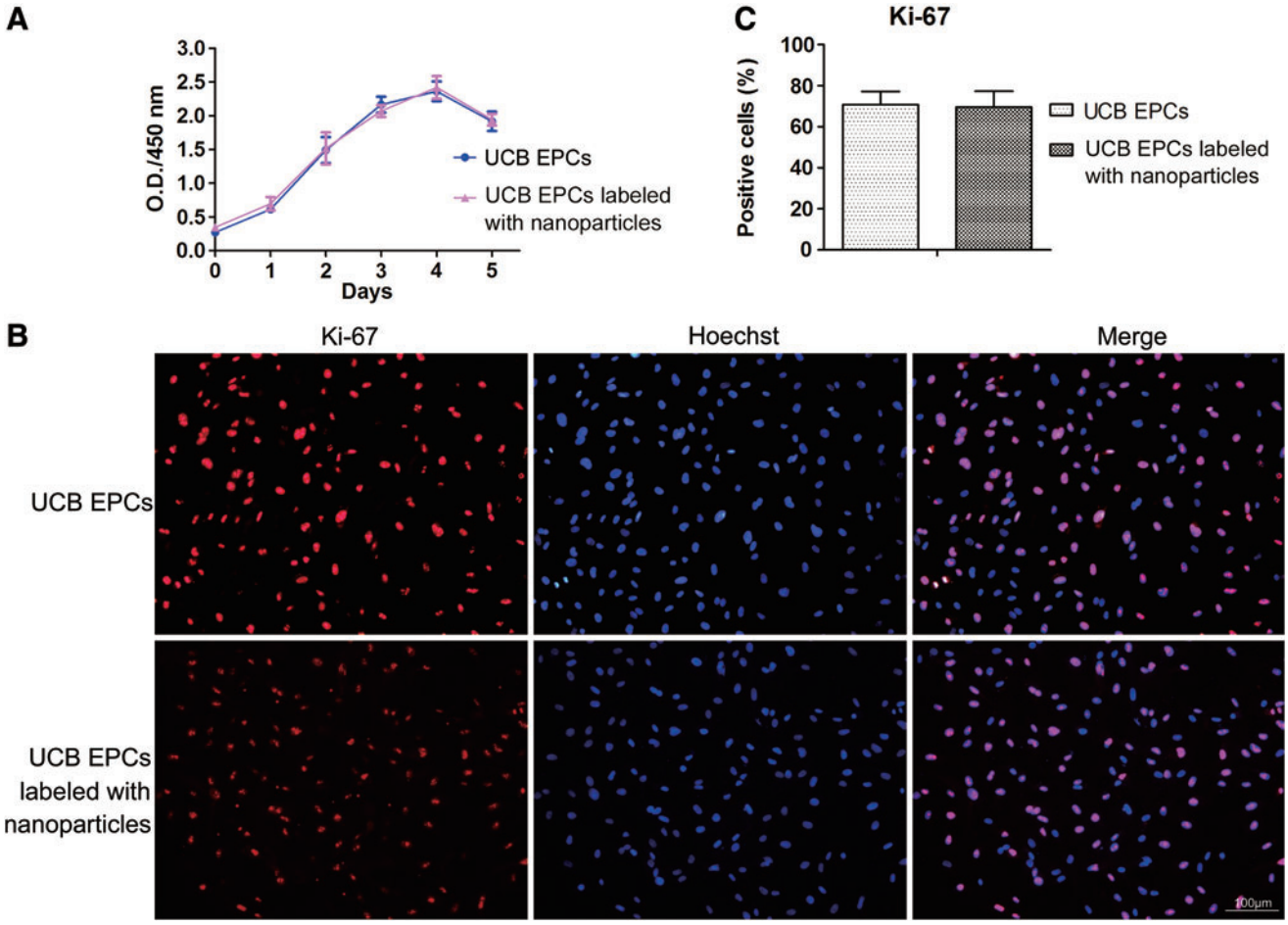

FIG. 5. Cell proliferation of human UCB EPCs after labeling with CD34 nanoparticles. **(A)** Cell counting kit-8 (CCK-8) assay for the proliferation of UCB EPCs labeled with and without CD34 nanoparticles in vitro culture for different days. The optical density (O.D.) values after 0, 1, 2, 3, 4, 5 days of culture showed that there was no significant difference in the proliferation between these two groups ($P > 0.05$). **(B)** Immunostaining analysis of Ki-67 (*red*) for UCB EPCs labeled with and without CD34 nanoparticles. Nuclei were stained with Hoechst (*blue*) (scale bar = 100 μm). **(C)** There was no significant difference in the Ki-67 positive cells between these two groups ($P > 0.05$). Color images available online at www.liebertpub.com/scd

immunomagnetic nanoparticles and the negative control groups ($P > 0.05$) (Fig. 5A).

Immunostaining demonstrated no significant differences in the Ki-67 expression between the UCB EPCs with or without CD34 immunomagnetic nanoparticle labeling (69.66% ± 7.67%, 70.77% ± 6.45%, respectively, $P > 0.05$) (Fig. 5B, C). The results of this study demonstrated that the immunomagnetic nanoparticles did not slow the cell proliferation.

In vitro attraction of UCB EPCs labeled with CD34 immunomagnetic nanoparticle with a magnet

The magnet could efficiently attract the UCB EPCs labeled with CD34 immunomagnetic nanoparticles antigravity to the upper side of the culture dish and formed a round morphology with a diameter of 15 mm. There was no difference between 2 and 24 h of magnet attraction (Fig. 6).

Evaluation of corneal appearance and thickness after transplantation

The corneas in the three groups showed obvious edema, and the cornea was thick 2 weeks after surgery (Fig. 7A). The rabbits in the CD34 immunomagnetic nanoparticle-labeled UCB EPCS and the magnet transplantation group (nano group) had minimal corneal opacity 4 months after surgery. The rabbits in the nanoparticle-labeled UCB EPCS without magnet transplantation group (the control group), and the EDM stripping but no injection of cells (the model group) had severe corneal opacities (Fig. 7B). The corneal thickness in the nano group was decreased from 1322.5 ± 187.9 μm 2 weeks postoperatively to 490 ± 21.6 μm 4 months postoperatively. The corneal thickness of the control group was decreased from 1517.5 ± 36 μm 2 weeks postoperatively to 832.5 ± 53.2 μm 4 months postoperatively, and the thickness in the model group was decreased from 1637.5 ± 45.7 μm 2 weeks postoperatively to 1,000 ± 14.2 μm 4 months postoperatively. Normal corneal thickness is 350 ± 18.3 μm (Fig. 7C).

Four months after surgery, the corneal edema score was significantly lower in the nano group (1 ± 0) than in the control group (3.5 ± 0.6) and the model group (3.8 ± 0.5) ($P < 0.001$) (Fig. 8A).

The corneal thickness in the nano group was significantly lower than in the control group ($P < 0.001$) and the model

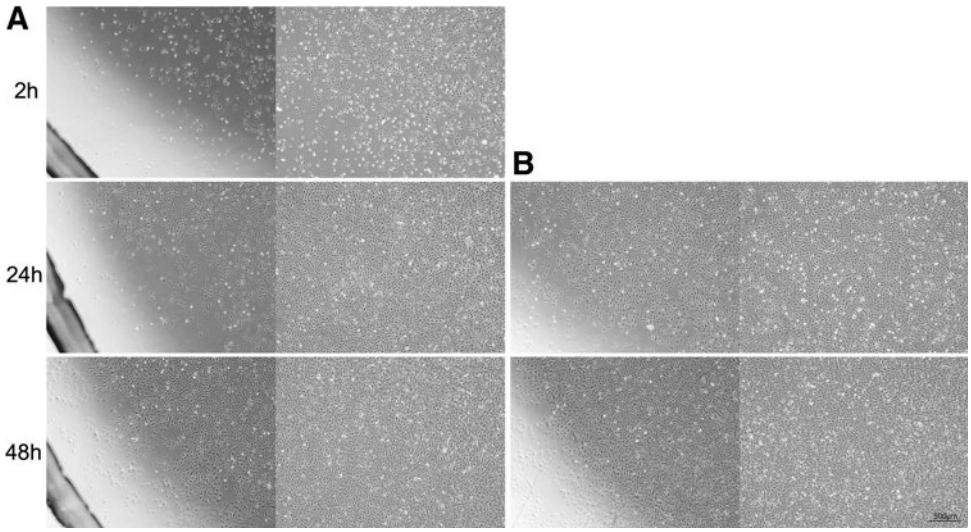

FIG. 6. In vitro attraction of human UCB EPCs labeled with CD34 immunomagnetic nanoparticles. **(A)** The nanoparticle-labeled UCB EPCs at different culture times after 2 h of magnet attraction. **(B)** The nanoparticle-labeled UCB EPCs at different culture times after 24 h of magnet attraction (scale bar = 500 μm).

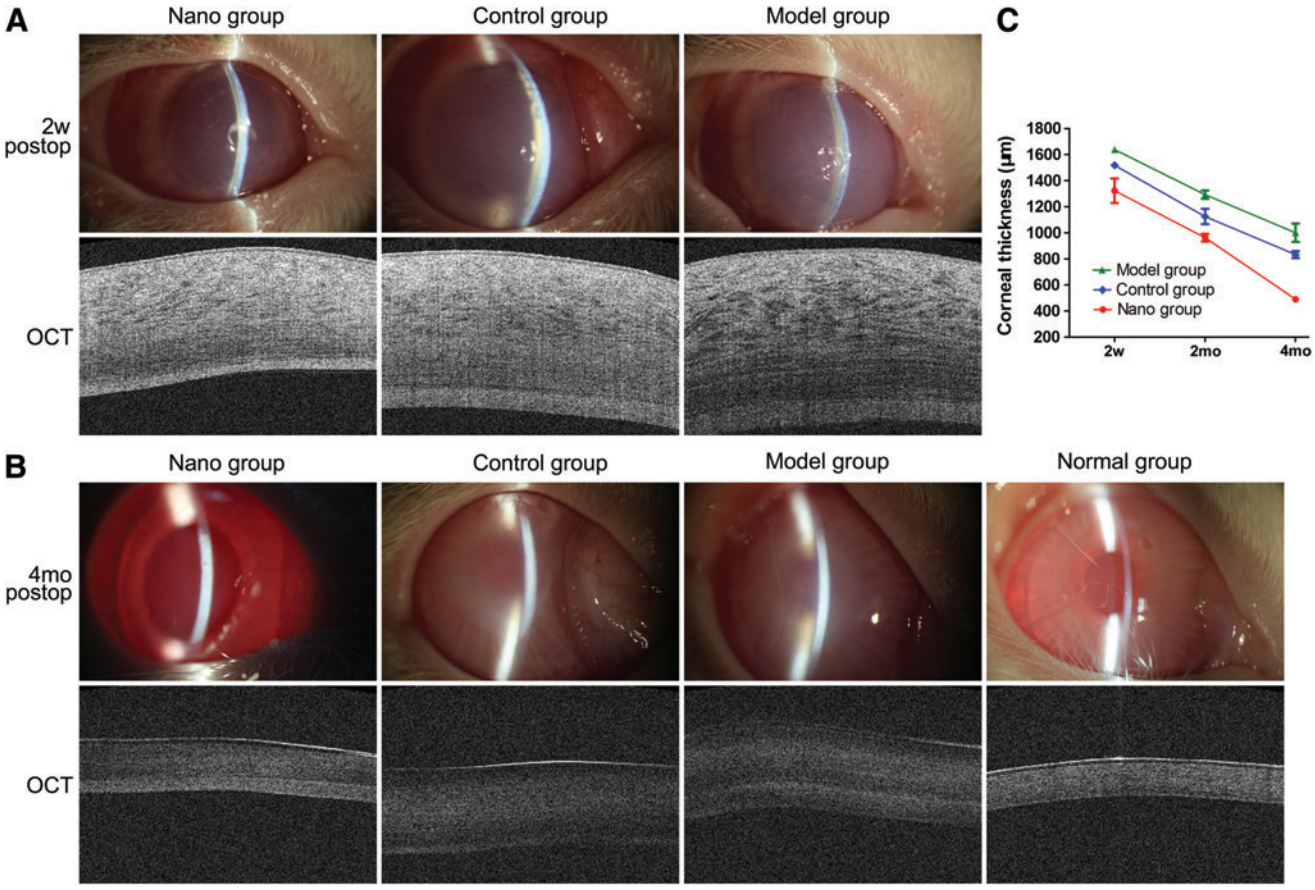

FIG. 7. Corneal appearance and thickness after transplantation. **(A)** Two weeks after surgery. The corneas had obvious edema with increased corneal thickness. **(B)** Four months after surgery. The corneas in the UCB EPCs labeled with nanoparticles and magnet attraction transplantation group (the nano group) had minimal corneal opacity, and the pupil and iris vessels were easily visible. The corneas in the nanoparticle-labeled UCB EPCS without magnet transplantation group (the control group) and the endothelium–Descemet membrane stripping, but no injection of cells (the model group) had severe corneal opacity, only pupil margin visible. OCT scan showed that the corneal thickness in the nano group was lower than in the control and the model group and similar to the normal group. **(C)** The corneal thickness decreased from 2 weeks to 4 months postoperatively in the nano, control, and model groups (2w, 2 weeks; 2mo, 2 months; 4mo, 4 months). Color images available online at www.liebertpub.com/scd

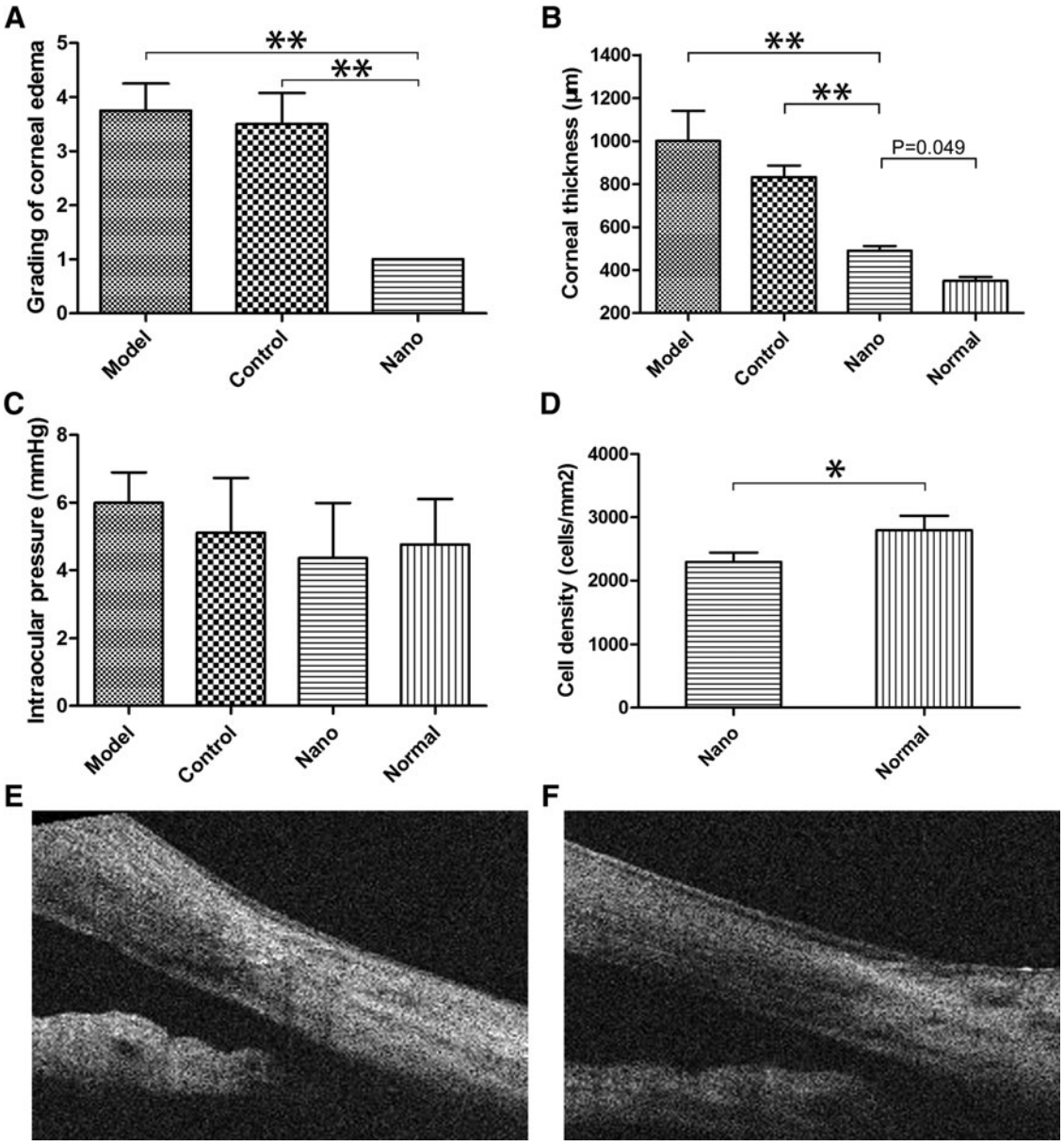

FIG. 8. Corneal edema grading, corneal thickness, intraocular pressure, endothelial cell density, and anterior chamber angle in the different groups 4 months postoperatively. **(A)** Grading of corneal edema. The corneal edema score was significantly lower in the nanoparticle-magnet group (1 ± 0) than in the control group (3.5 ± 0.6) and the model group (3.8 ± 0.5) ($^{**}P < 0.01$). **(B)** Corneal thickness. The corneal thickness in the nanoparticle-magnet group was significantly less than in the control group and the model group ($^{**}P < 0.01$) and similar to the normal group ($P = 0.049$). **(C)** Intraocular pressure. Compared with the intraocular pressure of the normal group, there was no significant difference in the other three groups ($P > 0.05$). **(D)** Endothelial cell density. The endothelial cell density in the nanoparticle-magnet group was lower than the normal group ($^{*}P < 0.05$). **(E)** Anterior chamber angle measured by OCT. OCT revealed an open anterior chamber angle and that no UCB EPCs clogged the angle in the nanoparticle-magnet group. **(F)** Normal anterior chamber of rabbit.

group ($P < 0.001$) and was close to the normal group (nano group vs. normal group, $P = 0.049$) (Fig. 8B).

Compared with the intraocular pressure of the normal group (4.76 ± 1.35 mmHg), there were no significant differences in the other three groups (nano group, 4.36 ± 1.63 mmHg, $P = 0.767$; control group, 5.11 ± 1.62 mmHg, $P = 0.858$; model group, 6 ± 0.89 mmHg, $P = 0.124$) (Fig. 8C).

The center corneal endothelial cell density in the nano group ($2{,}294 \pm 152$ cells/mm^2) was lower than in the normal group ($2{,}798 \pm 227$ cells/mm^2) ($P = 0.01$) (Fig. 8D). The center corneal endothelial cell density in the control group and the model group was not obtained.

OCT revealed an open anterior chamber angle, and no UCB EPCs clogged the angle in the nano group (Fig. 8E).

Histological examination after transplantation

The HE staining revealed a UCB EPC confluent monolayer attached tightly on the host corneal stroma in the nano group, and AQP1 immunoreactivity was detected. No inflammatory

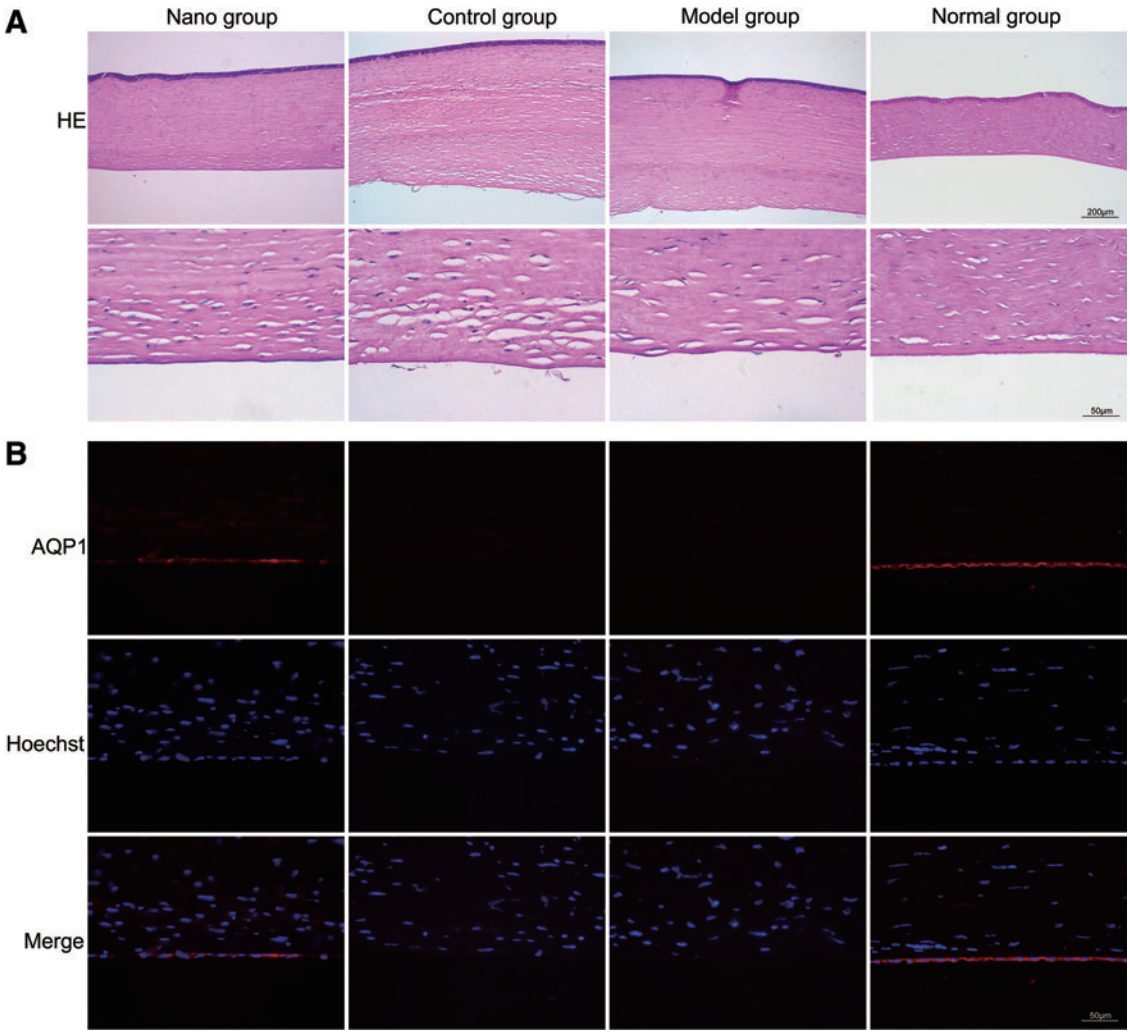

FIG. 9. Histological examination 4 months after transplantation. **(A)** The Hematoxylin and Eosin (HE) showed confluent UCB EPCs monolayers in the nanoparticle-magnet group (the nano group). The nanoparticle without magnet group (the control group) had few UCB EPCs on the host corneal stroma, and the model group had no corneal endothelial cells. **(B)** AQP1 immunoreactivity (*red*) was detected in the nano group and the normal group. Nuclei were stained by Hoechst (*blue*). Color images available online at www.liebertpub.com/scd

cells or neovascularization were observed. The control group had few UCB EPCs on the center of the host corneal stroma, and AQP1 immunoreactivity was not detected. The model group, in which the endothelium and Descemet's membrane were absent, showed marked stromal edema with no AQP1 expression. The normal cornea expressed AQP1 (Fig. 9A, B).

CM-Dil was tracked with weak red fluorescence, and human cell nuclei were stained by mouse anti-human nuclei monoclonal antibody with dark brown in the nano group, proving that the cells were transplanted UCB EPCs (Fig. 10A, B).

The Berlin blue staining for iron revealed no iron residue in the endothelium in the nano group (Fig. 10C, D).

Discussion

The corneal endothelial cells form a barrier between the cornea and the aqueous humor, helping to transport water from the corneal stroma, and maintaining corneal transparency through its barrier and ionic pump function. The human corneal endothelial cells (CECs) do not proliferate in vivo because they are arrested in the G1-phase of the cell cycle. Any loss or damage to the CECs is repaired by the spread of existing cells. When the cell density is reduced to below 400–500 cells per mm^2, the CECs could no longer adequately function, resulting in corneal edema, the development of bullous keratopathy, and the loss of visual acuity [12]. With the increasing worldwide shortage of corneas, stem cells, such as corneal endothelial precursor cells [13], corneal stroma stem cells [14], human embryonic stem cells [15], and human UCB mesenchymal stem cells [16], have been investigated to replace CECs. Putative EPCs were first isolated from human peripheral blood by magnetic bead selection on the basis of cell surface expression of the CD34 antigen [17]. EPCs could be isolated from human UCB [18], fetal livers or bone marrow by culturing sorted cells expressing the surface antigen CD34, CD133, vWF, and ingesting DiI-Ac-LDL or expressing antigens shared by hematopoietic and EPCs [19]. We previously reported that EPCs from the human fetus could transdifferentiate into corneal endothelial-like cells in vitro after coculture with CECs [3], but the obtaining of these cells is met with ethical issues.

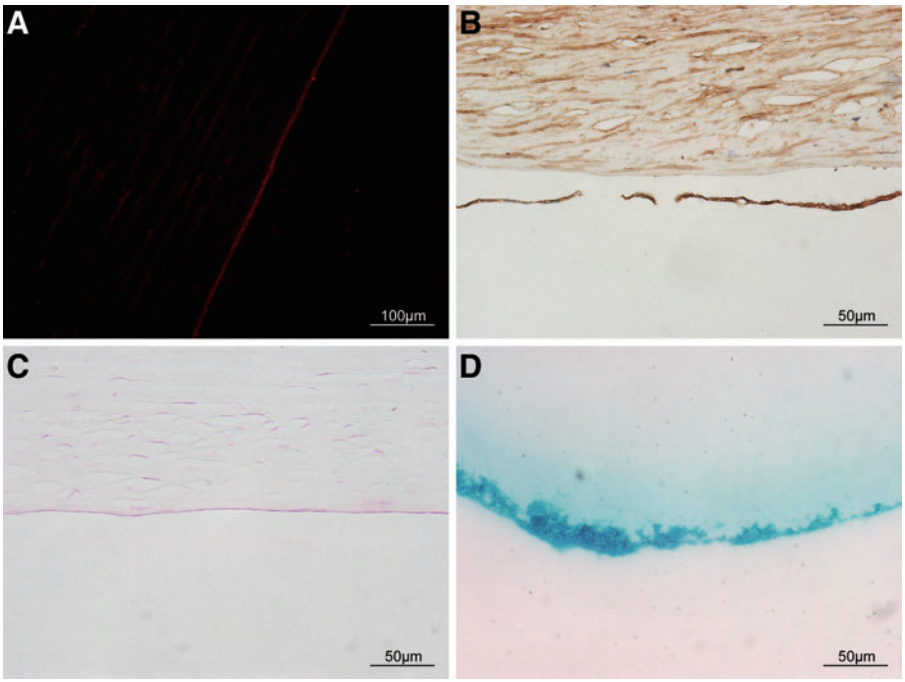

FIG. 10. Cell source and Berlin blue. **(A)** CM-Dil was tracked with weak *red* fluorescence in the nanoparticle with magnet group (scale bar = 100 μm). **(B)** Cell nuclei in the center corneal endothelium were stained by mouse anti-human nuclei monoclonal antibody with *dark brown* in the nanoparticle with magnet group (scale bar = 50 μm). **(C)** The Berlin blue staining for iron revealed no iron in the endothelium in the nanoparticle with magnet group (scale bar = 50 μm). **(D)** The Berlin blue staining was positive for the CD34 nanoparticles showing *blue* color (scale bar = 50 μm). Color images available online at www.liebertpub.com/scd

The current studies explore the feasibility of human UCB EPCs to repair corneal endothelial defects. UCB EPCs have several advantages over other stem cell sources for the following reasons: (i) Fewer moral and ethical issues than embryonic stem cells; (ii) EPCs from UCB are a younger type of stem cell than bone marrow, which could exhibit a decrease in the proliferative and differentiation capacity with donor age [16]. (iii) EPCs were enriched in UCB compared with adult peripheral blood. The number of EPCs per equivalent blood volume was increased 15-fold in cord blood compared with adult samples. EPCs from UCB contain higher levels of telomerase activity compared with adult samples [5]. (iv) With the increasing use of the Cord Blood Bank, autologous UCB EPCs transplantation would be easily achieved in the future, which can eliminate allogeneic rejection and would be safer. Moreover, EPCs obtained from cryopreserved UCBs were phenotypically and functionally indistinguishable from freshly isolated EPCs [20].

Various biological and synthetic scaffolds, such as decellularized corneal stroma [21], decellularized bovine corneal posterior lamellae [22], and silk fibroin membrane [23], have been used for corneal endothelium transplantation. Poor biocompatibility and degradation limit the application of these scaffolds. Attempts to transplant endothelial cells without biomaterial have been reported. A temperature-dependent culture system was used to reconstruct the endothelium, but it is difficult to manipulate during surgery [24]. Mimura transplanted iron-endocytozing cultured CECs with magnetic attraction to treat CEC defects. The drawback to this technique is that hemosiderosis might occur after the injection of iron-endocytozing CECs [10,25]. Bi attempted to use superparamagnetic iron oxide nanoparticle cell labeling to assist with HCEC transplantation by attaching the posterior corneal stroma in ex vivo animal models, but this has not been used for transplants in vivo [26].

Immunomagnetic nanoparticles, which refer to identification of the target antigen through capture antibodies conjugated onto the surface of magnetic particles. The most documented and currently the most useful application of magnetic nanoparticles is isolation and separation of specific molecules, which has been used in almost all areas of biosciences and biotechnology. A novel application of magnetic nanoparticles and magnetic force for tissue engineering, termed ''magnetic force-based tissue engineering (Mag-TE)'' has been proposed [27]. For medical use, especially for in vivo applications, it is of great importance that these particles do not have toxic effects or incompatibility with biological organisms. The noninvasiveness and simple nature of this method continues to enable the widespread use of magnetic particles [28,29].

In this study, we first proposed the application of immunomagnetic nanoparticles in the treatment of corneal endothelium defects. The UCB EPCs were specifically labeled with dextran-coated magnetic nanoparticles using bispecific TAC. These complexes recognize dextran and the cell surface antigen. The small size of the magnetic dextran iron particles allows for efficient binding to the TAC-labeled cells, through a fast, easy, and column-free cell isolation platform. The in vitro study showed that the nanoparticles did not alter the viability and proliferation of UCB EPCS. With the magnet attraction, the UCB EPCs labeled with nanoparticles could migrate directionally. In vivo, Berlin blue staining showed no residual iron in the endothelium. OCT revealed no cells or nanoparticles blocking the anterior chamber angle. The intraocular pressure was not increased. These results proved the effectiveness and safety of transplantations of UCB EPCs labeled with nanoparticles.

The white-to-white (corneal diameter), endothelial cell density, and CCT of New Zealand white rabbits are reported to be 13.5 mm, 3,000 cells/mm^2, and 373 μm, respectively [30,31]. The advantage of this designed magnet is that the magnetic force was well distributed on the area of the inner magnet, with a diameter of 15 mm, which was slightly larger than the rabbit corneal diameter, to ensure the attraction range. We developed a simple device filled with fluid to

simulate the anterior chamber, and turned over the culture dish to simulate anti-gravity. The in vitro study showed that the magnet could efficiently attract the UCB EPCs labeled with nanoparticles and distribute the cells uniformly. The UCB EPCs used in the in vitro and in vivo studies were calculated to be equivalent to the rabbit corneal endothelial cell density, which could ensure a sufficient cell number and avoid excess cells clogging the anterior chamber angle.

After transplantation, the corneas in the nanoparticle-magnet group showed little edema, and the corneas in the other group showed obvious edema. No immunological rejection has been detected. The corneal thickness in the nanoparticle-magnet group was close to the normal group. The UCB EPCs in the nanoparticle-magnet group could express AQP1, indicating that a pump function was established. These results indicate the UCB EPCs labeled with nanoparticles can move directionally in vivo and repair endothelium defects effectively. To the best of our knowledge, few published studies have described this technique. The advantage of this technique is fewer ethical issues, abundant stem cell resources, ease of manipulation, high safety, and no need for scaffolds, thereby avoiding poor biocompatibility and the degradation of scaffolds. This technique may be applied in clinic in the future.

The cornea did not become absolutely transparent during the follow-up time. We consider the following causes: (i) The follow-up time was not long enough; (ii) rabbits are not an optimal model for endothelial dysfunction. The rabbit cornea is too thin compared with the human cornea, and the anterior chamber is 2.08 ± 0.16 mm [32], which is too shallow for DMEK surgery to be performed without significant modification [33]; (iii) Descemet's membrane is the basement membrane of the corneal endothelium and helps keep the endothelial monolayer in place to maintain corneal clarity [34]. Rabbits regenerate their endothelium. If endothelium is stripped away alone without the Descemet membrane, the endothelial cells could quickly proliferate and repair the defects in the endothelium. So in this study, the Descemet's membrane was also stripped away. The absence of Descemet's membrane could keep the cornea from becoming clear. If this technique could be used in the clinic, the Descemet's membrane should not be stripped away, which might improve the results; (iv) The UCB EPCs might need to be differentiated into corneal endothelial cells first in vitro, which could launch the repair function immediately after transplantation. Recently, Hara et al. established a novel serum-free culture system for expanding human corneal endothelial progenitor cells (HCEPs) [35]. The HCEPs highly expressed p75 neurotrophin receptor, SOX9, and had a high proliferative potency. If the nanoparticle technique could be applied in HCEPs, the complete repair of cornea endothelium could be achieved with minimally invasive, easier to command, and avoiding the drawback of detachment of transplanted EDM sheet in DMEK surgery.

Conclusion

This study described a novel therapeutic method to repair corneal endothelium defects. In this work, human UCB EPCs were labeled with CD34 immunomagnetic nanoparticles, which could effectively be attracted directionally by a magnet in vitro in a self-made device simulating anterior chamber, and could be used to target to the host cornea stroma in vivo. The human UCB EPCs could repair corneal endothelial defects, providing a promising cell therapy for corneal endothelial dysfunction.

Acknowledgments

This work was supported by the National Natural Science Foundation of China grants (81370992), Shanghai Science and Technology Committee Foundation (11JC1407000, 12PJD025), Shanghai Jiao Tong University School of Medicine Doctor Innovation Found (BXJ201227), Shanghai Municipal Commission of Health and Family Planning Found (20144Y0221), and Shanghai Young Doctor Training Program.

Author Disclosure Statement

The authors report no conflicts of interest. The authors alone are responsible for the content and writing of the article.

References

1. Whitcher JP, M Srinivasan and MP Upadhyay. (1987). Corneal blindness: a global perspective. Bull World Health Organ 79:214–221.
2. Tourtas T, K Laaser, BO Bachmann, C Cursiefen and FE Kruse. (2012). Descemet membrane endothelial keratoplasty versus descemet stripping automated endothelial keratoplasty. Am J Ophthalmol 153:1082–1090.e2.
3. Shao C, Y Fu, W Lu and X Fan. (2011). Bone marrow-derived endothelial progenitor cells: a promising therapeutic alternative for corneal endothelial dysfunction. Cells Tissues Organs 193:253–263.
4. Paprocka M, A Krawczenko, D Dus, A Kantor, A Carreau, C Grillon and C Kieda. (2011). CD133 positive progenitor endothelial cell lines from human cord blood. Cytometry A 79:594–602.
5. Ingram DA, LE Mead, H Tanaka, V Meade, A Fenoglio, K Mortell, K Pollok, MJ Ferkowicz, D Gilley and MC Yoder. (2004). Identification of a novel hierarchy of endothelial progenitor cells using human peripheral and umbilical cord blood. Blood 104:2752–2760.
6. Xia J, M Luo, N Ni, J Chen, Y Hu, Y Deng, J Ji, J Zhou, X Fan and P Gu. (2013). Bone marrow mesenchymal stem cells stimulate proliferation and neuronal differentiation of retinal progenitor cells. PLoS One 8:e76157.
7. Deng Y, H Zhou, D Zou, Q Xie, X Bi, P Gu and X Fan. (2013). The role of miR-31-modified adipose tissue-derived stem cells in repairing rat critical-sized calvarial defects. Biomaterials 34:6717–6728.
8. Cammenga J, B Niebuhr, S Horn, U Bergholz, G Putz, F Buchholz, J Löhler and C Stocking. (2007). RUNX1 DNA-binding mutants, associated with minimally differentiated acute myelogenous leukemia, disrupt myeloid differentiation. Cancer Res 67:537–545.
9. Shao Y, L Quyang, Y Zhou, J Tang, Y Tan, Q Liu, Z Lin, T Yin, F Qiu and Z Liu. (2010). Preparation and physical properties of a novel biocompatible porcine corneal acellularized matrix. In Vitro Cell Dev Biol Anim 46:600–605.
10. Mimura T, S Yamagami, T Usui, Y Ishii, K Ono, S Yokoo, H Funatsu, M Araie and S Amano. (2005). Long-term outcome of iron-endocytosing cultured corneal endothelial cell transplantation with magnetic attraction. Exp Eye Res 80:149–157.

11. Arien-Zakay H, G Gincberg, A Nagler, G Cohen, S Liraz-Zaltsman, V Trembovler, AG Alexandrovich, I Matok, H Galski, et al. (2014). Neurotherapeutic effect of cord blood derived CD45 + hematopoietic cells in mice after traumatic brain injury. J Neurotrauma 31:1405–1416.
12. Joyce NC. (2012). Proliferative capacity of corneal endothelial cells. Exp Eye Res 95:16–23.
13. Yamagami S, T Mimura, S Yokoo, T Takato and S Amano. (2006). Isolation of human corneal endothelial cell precursors and construction of cell sheets by precursors. Cornea 25:S90–S92.
14. Hatou S, S Yoshida, K Higa, H Miyashita, E Inagaki, H Okano, K Tsubota and S Shimmura. (2013). Functional corneal endothelium derived from corneal stroma stem cells of neural crest origin by retinoic acid and Wnt/beta-catenin signaling. Stem Cells Dev 22:828–839.
15. Zhang K, K Pang and X Wu. (2014). Isolation and transplantation of corneal endothelial cell-like cells derived from in vitro-differentiated human embryonic stem cells. Stem Cells Dev 23:1340–1354.
16. Joyce NC, DL Harris, V Markov, Z Zhang and B Saitta. (2012). Potential of human umbilical cord blood mesenchymal stem cells to heal damaged corneal endothelium. Mol Vis 18:547–564.
17. Asahara T, T Murohara, A Sullivan, M Silver, R van der Zee, T Li, B Witzenbichler, G Schatteman and JM Isner. (1997). Isolation of putative progenitor endothelial cells for angiogenesis. Science 275:964–967.
18. Eggermann J, S Kliche, G Jarmy, K Hoffmann, U Mayr-Beyrle, KM Debatin, J Waltenberger and C Beltinger. (2003). Endothelial progenitor cell culture and differentiation in vitro: a methodological comparison using human umbilical cord blood. Cardiovasc Res 58:478–486.
19. Hristov M, W Erl and PC Weber. (2003). Endothelial progenitor cells: isolation and characterization. Trends Cardiovasc Med 13:201–206.
20. Lin RZ, A Dreyzin, K Aamodt, AC Dudley and JM Melero-Martin. (2011). Functional endothelial progenitor cells from cryopreserved umbilical cord blood. Cell Transplant 20: 515–522.
21. Choi JS, JK Williams, M Greven, KA Walter, PW Laber, G Khang and S Soker. (2010). Bioengineering endothelialized neo-corneas using donor-derived corneal endothelial cells and decellularized corneal stroma. Biomaterials 31:6738–6745.
22. Bayyoud T, S Thaler, J Hofmann, C Maurus, MS Spitzer, KU Bartz-Schmidt, P Szurman and E Yoeruek. (2012). Decellularized bovine corneal posterior lamellae as carrier matrix for cultivated human corneal endothelial cells. Curr Eye Res 37:179–186.
23. Madden PW, JN Lai, KA George, T Giovenco, DG Harkin and TV Chirila. (2011). Human corneal endothelial cell growth on a silk fibroin membrane. Biomaterials 32:4076–4084.
24. Hsiue GH, JY Lai, KH Chen and WM Hsu. (2006). A novel strategy for corneal endothelial reconstruction with a bioengineered cell sheet. Transplantation 81:473–476.
25. Mimura T, N Shimomura, T Usui, Y Noda, Y Kaji, S Yamgami, S Amano, K Miyata and M Araie. (2003). Magnetic attraction of iron-endocytosed corneal endothelial cells to Descemet's membrane. Exp Eye Res 76:745–751.
26. Bi YL, MF Wu, LX Lu, Q Zhou, F Du, XT Sun, SF Tang and GT Xu. (2013). Functions of corneal endothelial cells do not change after uptake of superparamagnetic iron oxide nanoparticles. Mol Med Rep 7:1767–1772.
27. Ito A, M Shinkai, H Honda and T Kobayashi. (2005). Medical application of functionalized magnetic nanoparticles. J Biosci Bioeng 100:1–11.
28. Alexiou C, R Jurgons, C Seliger and H Iro. (2006). Medical applications of magnetic nanoparticles. J Nanosci Nanotechnol 6:2762–2768.
29. Park H, MP Hwang and KH Lee. (2013). Immunomagnetic nanoparticle-based assays for detection of biomarkers. Int J Nanomedicine 8:4543–4552.
30. Wang X, J Dong and Q Wu. (2014). Mean central corneal thickness and corneal power measurements in pigmented and white rabbits using Visante optical coherence tomography and ATLAS corneal topography. Vet Ophthalmol 17:87–90.
31. Jee DH and HS Kim. (2010). The effect of C(3)F(8) gas on corneal endothelial cells in rabbits. Jpn J Ophthalmol 54: 602–608.
32. Yuksel H, FM Turkcu, S Ari, Y Cinar, AK Cingu, M Sahin, A Sahin, Z Ozkurt and I Caça. (2014). Anterior segment parameters of rabbits with rotating Scheimpflug camera. Vet Ophthalmol. DOI: 10.1111/vop.12150.
33. Niu G, JS Choi, Z Wang, A Skardal, M Giegengack and S Soker. (2014). Heparin-modified gelatin scaffolds for human corneal endothelial cell transplantation. Biomaterials 35:4005–4014.
34. Chow VW, T Agarwal, RB Vajpayee and V Jhanji. (2013). Update on diagnosis and management of Descemet's membrane detachment. Curr Opin Ophthalmol 24: 356–361.
35. Hara S, R Hayashi, T Soma, T Kageyama, T Duncan, M Tsujikawa and K Nishida. (2014). Identification and potential application of human corneal endothelial progenitor cells. Stem Cells Dev 23:2190–2201.

Address correspondence to:
Prof. Xianqun Fan
Department of Ophthalmology
Ninth People's Hospital
Shanghai Jiao Tong University School of Medicine
No. 639 Zhi Zao Ju Road
Shanghai 200011
China

E-mail: fanxq@sh163.net

Prof. Yao Fu
Department of Ophthalmology
Ninth People's Hospital
Shanghai Jiao Tong University School of Medicine
No. 639 Zhi Zao Ju Road
Shanghai 200011
China

E-mail: fuyaofy@sina.com

Received for publication May 21, 2014
Accepted after revision October 11, 2014
Prepublished on Liebert Instant Online October 15, 2014